JOURNAL OF MATERIALS SCIENCE 4 (1969) 359–369

An Experimental Investigation of the Structure of some Internally Oxidised Ferromagnetic Alloys

R. BARLOW, P. J. GRUNDY, B. JOHNSON
Department of Pure and Applied Physics, University of Salford, Salford 5, Lancs, U K

Received 31 July 1968 and in revised form 13 January 1969

Results are presented of optical, scanning electron and transmission electron microscope observations on some internally oxidised ferromagnetic alloys. The alloys investigated were of nominal composition 0.058 wt % Si in Ni, 0.48 wt % Si in Ni and 0.17 wt % Si in Co 66.2%–Ni 33.7%. The alloys were in polycrystalline form and in addition single crystals of 0.058 wt % Si in Ni were examined. The diffusion and oxidation rate constants are calculated and the state of the oxide product as a function of (i) depth in the alloy, (ii) oxidising temperature and (iii) alloy composition is considered. The possibility of using such systems as device material and as test material for theories of coercivity and approach to magnetic saturation is considered.

1. Introduction

One of the major contributions to coercivity in ferromagnetic materials is from domain wall-inclusion interactions. Several theories for this particular contribution have been put foward [1-4]. The approach to magnetic saturation is also affected by inclusions [5-7]. An experimental test of such theories should involve the preparation of a well defined precipitate system in a ferromagnetic matrix. As suggested in a previous publication [8] internal oxidation of binary alloys containing small amounts of silicon is a possible method of producing dispersed and inert spheroidal non-magnetic precipitates. Several workers have investigated internal oxidation processes in solid and compacted Cu-Si alloys [9-11] and Ni-Si alloys [12] in connection with the dispersion-strengthening of materials. Transmission electron microscopy was used by Ashby and Smith [9] and replica electron microscopy by Bolsaitis and Kahlweit [11] and Bonis and Grant [12]. The work reported here is a structural investigation of internal oxidation in Ni–Si and Co–Ni–Si alloys with the aim of preparing the optimum system for magnetic investigation. As recently reported [13], such systems have possible applications as a mechanically stabilised magnetic material.

Ferromagnetic alloys based on nickel were chosen for this investigation because they internally oxidise readily. A high proportion of cobalt was used in one alloy in an attempt to internally oxidise a system with a relatively high saturation magnetisation value and Curie temperature. A nickel content just greater than 32 wt % in this alloy suppresses the phase change from an fcc to an hcp structure which occurs in pure cobalt at about 420° C and which may be affected by precipitation of incoherent silica particles. It is hoped to investigate at a later date the internal oxidation process in Co–Si, with the aim of studying any possible modification of the dislocation-induced shear mechansim.

2. Specimen Preparation

If a dilute alloy, in which the solute (B) has a greater affinity for oxygen than the solvent (A), is heated in an oxidising atmosphere, oxygen may diffuse into the alloy, react with solute B, and cause an oxide of B to be precipitated in the parent matrix. This process is called internal oxidation and offers a convenient method of obtaining a dispersed oxide in a pure metal matrix.

Discs of 3 mm diameter, thickness 100 to 500 μm, obtained by spark-machining, were intern-

ally oxidised for various times and at several temperatures by heating them in a "Rhines pack" [14], composed of two parts $NiO–Ni_2O_3$, one part Ni and one part Al_2O_3, in a closed silica tube. In the case of single crystal discs the faces were cut parallel to a (100) plane. For the cobalt-nickel alloy the pack used was composed of two parts $CoO–Co_2O_3$, one part Co and one part Al_2O_3. In this "Rhines pack" the partial pressure of oxygen is maintained at the dissociation pressure of the lowest oxide of the base metal so that only the oxide of the less noble solute element can be formed. The discs were thinned for transmission electron microscopy by a jet electropolishing technique. In this method the discs are jet-polished from both sides so that an area at any required depth from the surface of the specimen could be examined, the depth measurements being made by optical microscopy. Transmission electron microscopy was carried out in a Hitachi HU11A microscope at an operating voltage of 100 kV.

The penetration depth of the oxidation front was measured using an optical microscope after the discs had been embedded in a plastic material, sectioned, mechanically polished and finally electropolished. The sectioned and electropolished discs were coated with a thin layer of gold/palladium before examination in the Stereoscan scanning electron microscope.

3. Experimental Results

3.1. Single Crystal Ni–0.058 wt % Si Alloy

The rates of penetration of the oxidation front for temperatures in the range 800 to 1200° C have been measured. At 830° C the front is seen as a distinct plane parallel to the specimen surface but as the temperature, and so the rate of penetration, is increased the front becomes less well-defined making the depth measurement more difficult. The variation of the square of the depth of penetration with time for various temperatures is shown in fig. 1. It is evident that in this temperature range the rate of diffusion of oxygen in nickel is markedly increased for small increases in temperature. The temperature dependence of the depth of the internally oxidised zone in this and the other alloys investigated was observed to follow a parabolic rate law of the form

$$\frac{X^2}{t} = \mathrm{B} \exp\left(-\frac{\mathrm{C}}{T}\right) \qquad (1)$$

where X is the thickness of the internally oxidised zone, t is the time of oxidation, T is the absolute temperature and B and C are constants characteristic of a given alloy. Under conditions similar to those which are assumed to exist in the internal oxidation process (a concentration gradient of oxygen from the surface region of the alloy where the oxygen concentration is at the solubility limit) Fick's law may be written as

$$\mathrm{D} = \frac{X^2}{t} \qquad (2)$$

where D is the diffusion coefficient of the oxidation front at a particular temperature. Equations 1 and 2 may thus be combined in the form of the well-known diffusion law

$$\mathrm{D} = \mathrm{D_c} \exp\left(-\frac{\mathrm{Q}}{\mathrm{R}T}\right) \qquad (3)$$

where here D_c and Q/R are identified as B and C of equation 1, Q is an activation energy for diffusion and R is the gas constant. For this alloy D_c and Q are computed from a plot of $\ln X^2/t$ against $1/T$ (fig. 2) as 9.67×10^3 cm²/sec and 70.91 kcal/g atom respectively, as shown in table I.

For the calculation of expected penetration depths or oxidation times in internal oxidation the rate law can also be expressed as

$$\ln \frac{X^2}{t} = -\frac{\mathrm{a}}{T} + \mathrm{b}$$

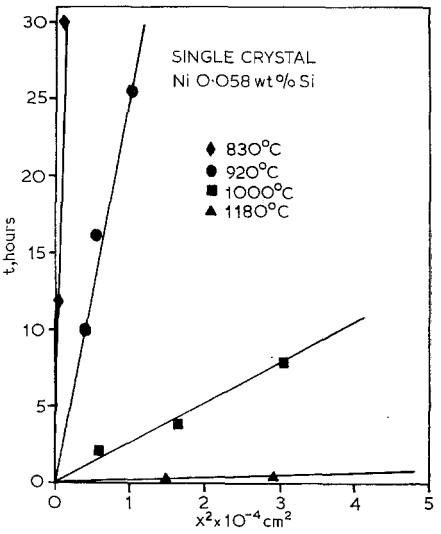

Figure 1 Relationship between time of oxidation t and thickness of zone of internal oxidation X for the single crystal nickel–0.058 wt % silicon alloy.

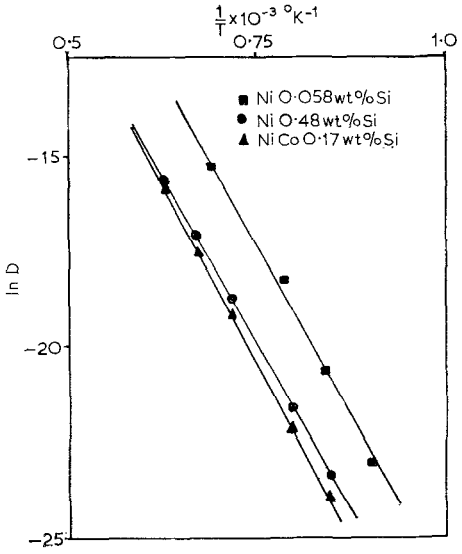

Figure 2 Relationship between the logarithm of the diffusion coefficient D and the reciprocal of the absolute temperature $1/T$ for the three alloy systems investigated.

where a and b are constants [15, 16]. For convenience these are also given in table I (X is expressed in cm, t in sec).

The size and shape of the amorphous silica particles precipitated were found to be dependent upon the temperature of oxidation and their depth below the specimen surface. At all temperatures the particles precipitated just below the specimen surface are mainly spherical with a size variation in the range 0.2 to 0.5 μm. The average particle size increases with the depth of penetration of the oxidation front, being 0.6 to 0.8 μm at 100 μm and approximately 1.0 μm at 200 μm. At 1200° C the particles have a much broader size distribution than at any other temperature. The particles produced at 830° C have no definite shape whilst those produced at 920° C are cuboidal, those at 1000° C are a mixture of cubes and spheres (fig. 3) and those at 1200° C are spherical (fig. 4). Thin films of silica have been observed to form at all depths in specimens oxidised at the lowest temperatures. These films are in general amorphous although infrequently they are crystalline, as determined by electron diffraction.

An optical examination of the jet electropolished discs has revealed that the oxide is preferentially precipitated on discontinuities, e.g. twin-boundaries in the metal matrix.

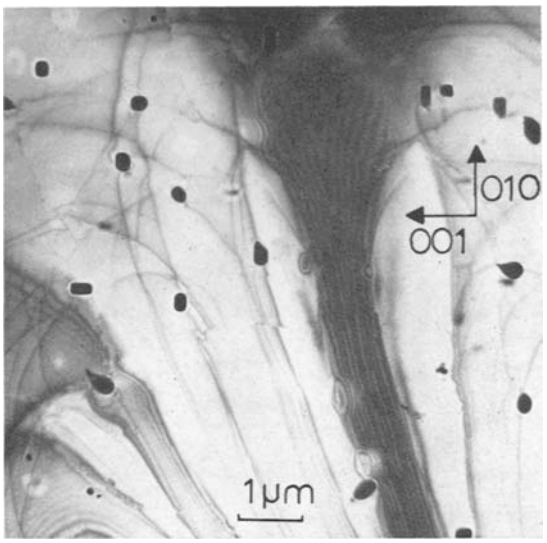

Figure 3 Disc of single crystal nickel–0.058 wt % silicon, internally oxidised at 1010° C, showing different shaped precipitates. Transmission electron micrograph (TEM).

3.2. Polycrystalline Ni–0.058 wt % Si Alloy

Discs of this alloy were obtained from cold-rolled slices of the single crystal, vacuum-annealed at 600° C to give an average grain size of 150 μm. The presence of grain-boundaries has a considerable effect on the penetration rate of the oxidation front. At 800° C the precipitation of silica takes place mainly at grain-boundaries which suggests that the diffusion of oxygen is principally along these boundaries. Between 900 and 1000° C the rate of oxygen diffusion along the boundaries is slightly greater than the rate of diffusion in the grains. For a 25 h oxidation at 925° C the penetration depth of the oxidation

TABLE I

Alloy	D_0 (cm^2/sec)	Q (kcal/g atom)	a (° K)	b
Ni–0.058 wt % Si	$9.67 \pm 0.95 \times 10^3$	70.91 ± 2.28	$3.55 \pm 1.14 \times 10^4$	9.18 ± 0.90
Ni–0.48 wt % Si	$1.51 \pm 0.07 \times 10^3$	71.56 ± 0.88	$3.58 \pm 0.44 \times 10^4$	7.32 ± 0.37
Ni–Co–0.17 wt % Si	$3.72 \pm 0.25 \times 10^3$	75.13 ± 1.84	$3.76 \pm 0.92 \times 10^4$	8.22 ± 0.55

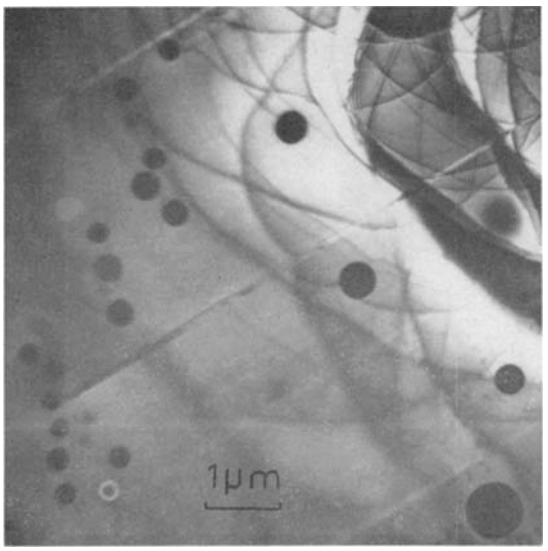

Figure 4 Disc of single crystal nickel–0.058 wt % silicon, internally oxidised at 1200° C, showing spherical silica particles (TEM).

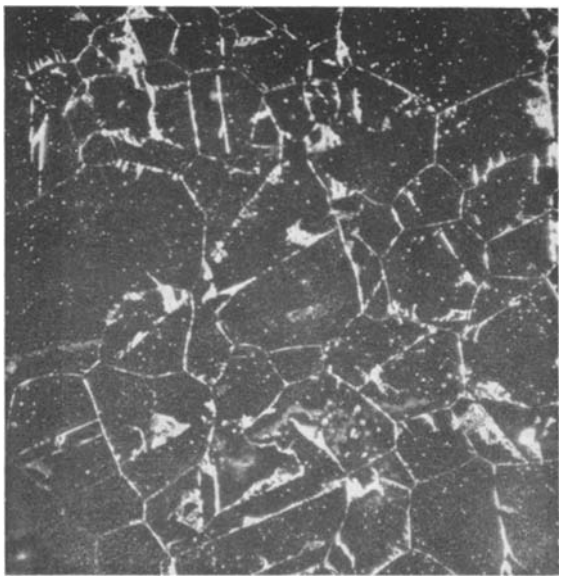

Figure 5 Optical micrograph of a disc of polycrystalline nickel–0.058 wt % silicon, internally oxidised at 925° C, showing localised networks of silica and grain-boundary precipitation (× 77).

front is 125 μm compared to 100 μm in the single crystal.

In addition to the normal form of precipitate, localised irregular networks of silica are observed at depths greater than about 40 μm. The optical micrograph of fig. 5 shows these networks as film-like structures at sites on the grain-boundaries. The silica particles formed in the grains are mainly spherical with a size range 0.2 to 0.3 μm. The cuboidal particles that are present have faces parallel to particular planes in the nickel matrix, e.g. they appear cubic in {100} oriented grains and hexagonal in {111} oriented grains (see figs. 3 and 8b). The particles in the grain-boundaries are spherical or lenticular with a size variation in the range 0.1 to 0.3 μm dependent upon the grain misorientation across the boundaries. Optical microscopy reveals that there is preferential precipitation on the grain-boundaries, as can be seen in the low magnification micrograph of fig. 5.

Above 1000° C enhanced grain-boundary diffusion of oxygen occurs at the expense of diffusion in the grains. At 1180° C the rate of penetration of the oxidation front through the grain is half that of the single crystal case. At this temperature no localised networks are present (fig. 6), the oxidation product being solely spherical and lenticular silica particles. The size of the particles precipitated on the grain-boundaries does not vary to any great extent with depth below the surface but the dependence on boundary misorientation produces a size variation of 0.1 to 0.5 μm (fig. 7). The size of the particles in the grains increases not only with

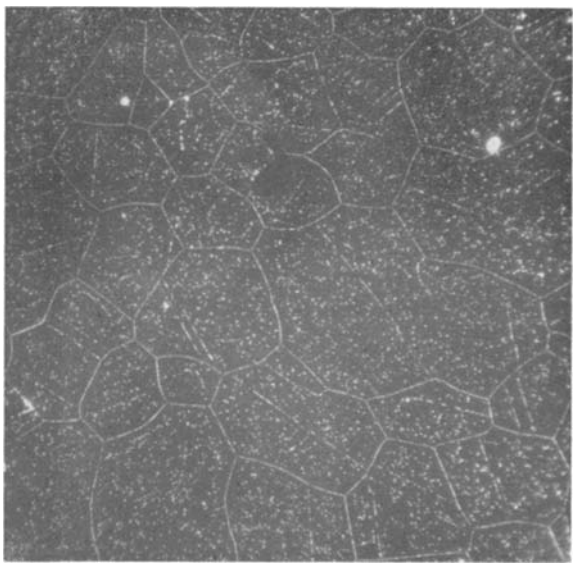

Figure 6 Optical micrograph of a disc of polycrystalline nickel–0.058 wt % silicon, internally oxidised at 1180° C, showing preferential grain-boundary and twin-precipitation (× 77).

depth but also with grain size. However, the particles are smaller than in the single crystal material, being ~ 0.2 μm near the surface and ~ 0.5 μm at a depth of 100 μm for a grain of average size. The preferential grain-boundary twin-precipitation is clearly visible optically after the jet electropolishing (fig. 6).

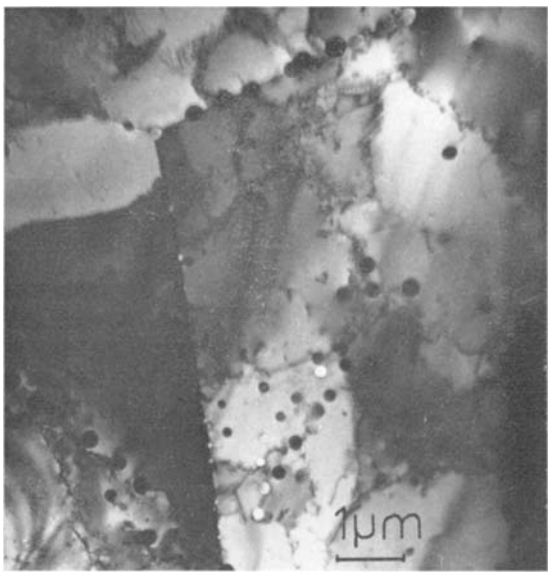

Figure 7 Disc of polycrystalline nickel–0.058 wt % silicon, internally oxidised at 1200° C, showing precipitation on grain-boundaries (TEM).

If the average grain size is reduced to 50 μm or less by oxidising cold-rolled, unannealed alloy the precipitation of the silica takes place mainly at the grain-boundaries. For oxidation between 900 and 1000° C dense arrays of particles are formed at the boundaries (fig. 8a) and in certain cases the precipitate is aligned in filaments across the boundaries (fig. 8b). The localised network formation which takes place in the large-grained material is drastically reduced but structures, which are similar in form to dendrites and to structures observed in Cu–Si alloys internally oxidised between 700 and 800° C [11], are occasionally precipitated around the grain-boundaries (fig. 9).

3.3. Polycrystalline Ni–0.48 wt % Si Alloy

The rate of penetration of the oxidation front for temperatures in the range 900 to 1300° C have been measured. At all temperatures the front is a distinct plane parallel to the specimen surface and the grain-boundaries have little or no effect on the penetration depth. The variation of the square of the depth of penetration with time for various temperatures is shown in fig. 10 and the constants of diffusion and oxidation, D_c, Q, a and b for this alloy are shown in table I.

The structure of the oxidation product varies with the depth of penetration, being firstly in the form of spherical particles, whose size varies from 0.2 to 2.0 μm, and then a mixture of

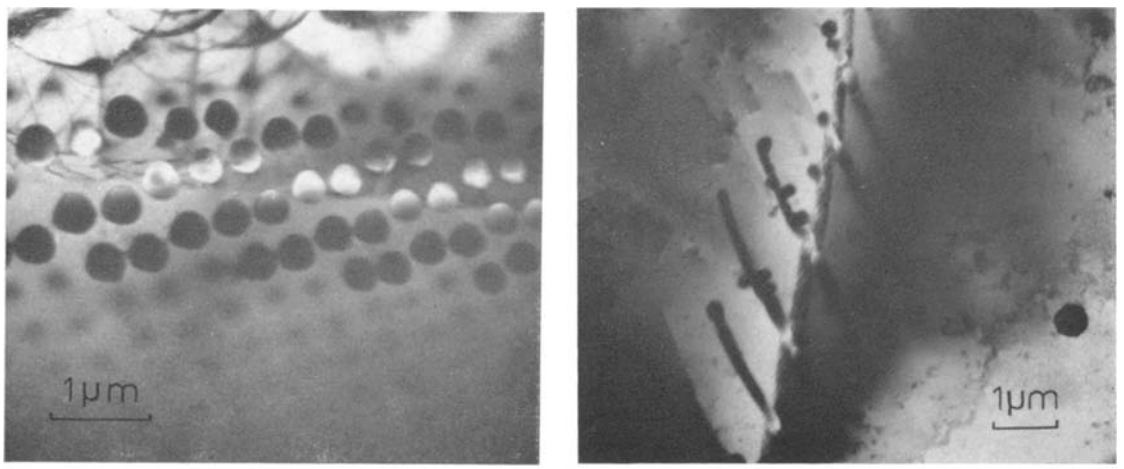

(a) (b)

*Figure 8*a Thin foil of small grained nickel–0.058 wt % silicon, internally oxidised at 920° C, showing arrays of silica particles across the grain-boundaries (TEM). b Thin foil of small grained nickel–0.058 wt % silicon, internally oxidised at 900° C, showing filaments of silica across the grain-boundaries (TEM).

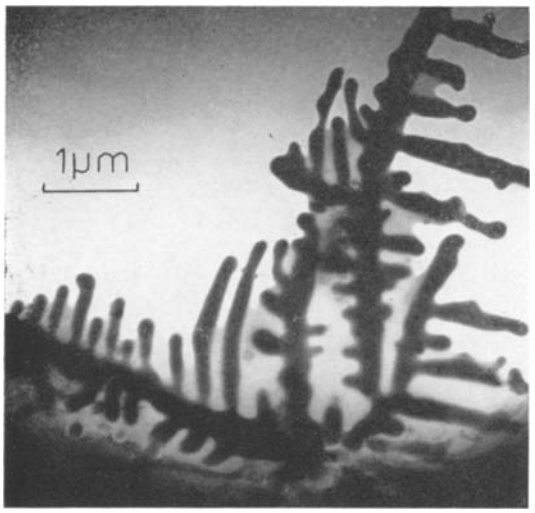

Figure 9 Thin foil of small grained nickel–0.058 wt% silicon, internally oxidised at 920° C, showing "dendrites" of silica (TEM).

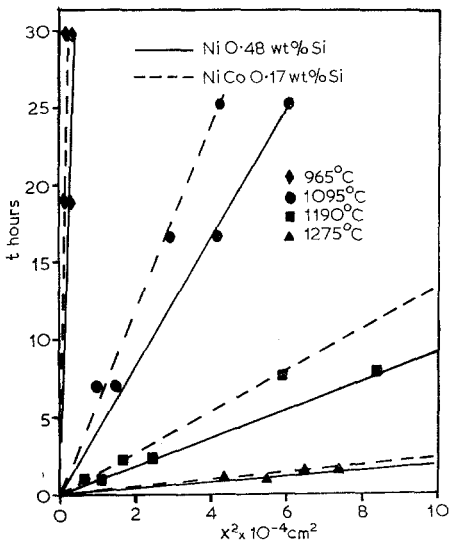

Figure 10 Relationship between time of oxidation t and thickness of zone of internal oxidation X for the nickel–0.48 wt % silicon and nickel (33.7%)–cobalt (66.2%)–0.17 wt % silicon alloys.

particles, filaments and networks of silica. The depth of the particulate zone increases with increasing temperature and the structure of the precipitate below this zone becomes predominantly filamentary. At 950° C the particles extend only to a depth of a few μm while at 1280° C the depth is approximately 75 μm. The grain-boundaries are saturated with precipitate and as in the Ni–0.058 wt % Si alloy the networks form around the boundaries but do not extend into the grains to the same extent. Most of the silica is precipitated as side-branched filaments which have a length variation of 1 to 20 μm, a mean diameter of 0.75 μm and are all parallel to each other within a grain (fig. 11a, b). The ends of the filaments and their side branches are rounded and have approximately the same diameter as the particles present. Selected area electron diffraction shows that these filaments lie in {100} planes of the nickel matrix.

Thin films of amorphous silica have been observed between the branches of the networks below 1200° C, similar to those in fig. 9.

3.4. Polycrystalline NiCo–0.17 wt % Si Alloy

The variation of the square of the depth of penetration of the oxidation front with time for temperatures in the range 900 to 1300° C is shown in fig. 10 and the constants of oxidation for this alloy system are again tabulated in table I. The oxidation front is not as distinct as in the Ni–0.48 wt % Si alloy because at some depth below the specimen surface the structure of the precipitate changes from particles to extended structures of silica which are typically dendritic in form (fig. 12a, b). The depth at which the structure changes is temperature-dependent and varies from about 25 μm at 1000° C to about 100 μm at 1300° C. The change in structure and the slight enhancement of the oxygen diffusion along grain-boundaries at the higher temperature causes some uncertainty in the measurement of the penetration depth.

Electron microscopy shows that the particle size varies from 0.2 to 1.0 μm, and that the mean diameter increases from 0.5 μm at or near the surface to 1.0 μm at a depth slightly less than that at which the structure change occurs. The effect of increasing temperature is to reduce the mean particle size at any given depth. There is little preferential precipitation of silica at the grain-boundaries before the structure change and the particles which are precipitated on the boundaries have a mean size which is approximately half that of the particles precipitated in the grain. The particle shape is spherical in the grain and spherical and lenticular on the grain-boundaries.

The extended structures or "dendrites" precipitated at the greater depths are shown in fig. 12b and at these depths the grain-boundaries are saturated with precipitate.

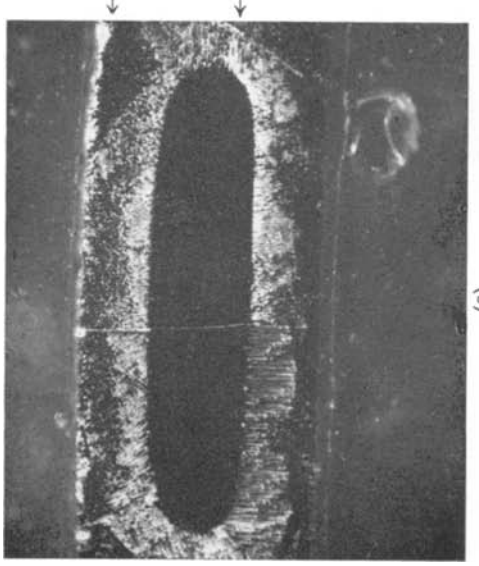

Figure 11a Optical micrograph of sectioned disc of nickel–0.48 wt % silicon, internally oxidised at 1175° C, showing structure of oxidation product (× 68). b Scanning electron micrograph of sectioned disc of nickel–0.48 wt % silicon, internally oxidised at 1175° C, showing the structure of the oxidation product (× 233).

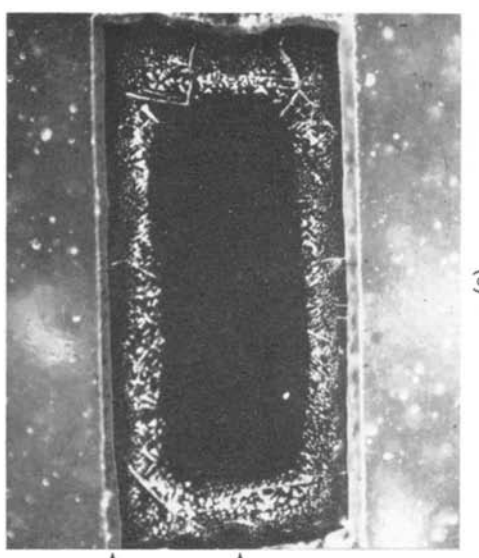

Figure 12a Optical micrograph of sectioned disc of nickel–cobalt–0.17 wt % silicon, internally oxidised at 1175° C, showing structure change of oxidation product with depth (× 68). b Scanning electron micrograph of section disc of nickel–cobalt–0.17 wt % silicon, internally oxidised at 1175° C, showing the change of structure with depth (× 116).

4. Discussion

The values of D_c and Q, obtained from fig. 2 and presented in table I, for the three alloy systems that have been studied, allow some probable conclusions to be drawn on the factors governing the growth rate of the internally oxidised zone. It can be seen, from this table and the gradients of the curves in fig. 2, that the values of Q for the two Ni-based alloys are little different; thus it would appear that solute concentration, at these levels, has only a small effect on the activation energy for interstitial diffusion of oxygen. The small increase in Q for the higher silicon content may be due to a contribution from a possible impeding effect of precipitated silica. The rate of advancement of the oxidation front is essentially controlled by the value of D_c at a particular temperature. The decrease in D_c for the higher solute content alloy is due to the increased absorption of oxygen, assuming that the solubility and the diffusion rate of oxygen is unaffected. The impeding effect of precipitated oxidation product would also tend to reduce D_c. A quantitative comparison of the two values of D_c cannot be made because the 0.48 wt % Si alloy contains grain-boundaries which may affect the advancement of the oxidation front. Also it will be pointed out later that the precipitation of silica is a vacancy-controlled mechanism so that the concentration of vacancies at, and the rate of supply of vacancies to, the oxidation front will be a determining factor in the rate at which the oxidised zone grows. The value of Q obtained for the Ni-Co-based alloy shows that the energy barrier for oxygen diffusion is higher than in the Ni-based alloys. As expected, because of the smaller solute content, the diffusion constant D_c is greater than in the Ni–0.48 wt % Si alloy. However, the oxidation rate is less and it would appear that the increase in activation energy is the main reason for this, although grain-boundary and vacancy concentration and mobility factors may make some unknown contribution.

The formation of a highly dispersed oxide product requires a large diffusion rate of oxygen relative to that of silicon. As the smallest mean particle size obtainable in the single crystal Ni–0.058 wt % Si alloy is 0.2 to 0.5 μm it is evident that the diffusion rate of oxygen is not much greater than that of silicon. This is supported by the observations that the particle size increases with depth of penetration and that an increase in temperature results in an increase in the size variation.

The diffusion rate, D_{Si}, of silicon in a Ni–Si alloy containing less than 1 wt % Si has been calculated, from data abstracted by Smithells [17], using a diffusion equation of the form

$$D_{Si} = D_c \exp - \frac{Q}{RT},$$

to be 9.0×10^{-10} cm^2/sec at 1180° C. The diffusion rate, D_O, for oxygen in nickel at 1180° C is obtained as 5.9×10^{-7} cm^2/sec from equation 3 of Rhines *et al* [15] by substitution of the value $X^2/t = 2.25 \times 10^{-7}$ cm^2/sec determined from fig. 1. A ratio of D_O/D_{Si} is thus obtained as 0.65×10^3.

Previous work [9 to 11] has shown that a dispersed oxide product is easily obtainable in Cu–Si alloys. The ratio of the oxygen and silicon diffusion rates in copper at 800° C has been calculated to be of the order of 1.5×10^4, using data given by Smithells [17] for silicon in copper and by Bolsaitis and Kahlweit [11] for oxygen in copper.

Silicon dissolves in nickel substitutionally and oxygen is assumed to dissolve interstitially so that when silicon and oxygen react to form silica there is an increase in volume. Unless this volume is accommodated by mass transfer of nickel atoms, large compressive strains will develop in the matrix around the silica particles making them grow fastest along those directions in the matrix which allow the smallest rate of increase of strain energy. These are the <100> directions in nickel [18]. It is assumed that when the particles are spherical any strain which would arise through an increase in volume is avoided by the absorption of vacancies at the particle/matrix interface, i.e. the strain anneals out as it forms. Strains produced during cooling of the alloy due to differences in thermal expansion coefficient of the particles and the matrix are minimised by furnace-cooling the specimens. No evidence of strain contrast of the thermal expansion type [19] has been observed in the electron micrographs taken, in any Bragg reflection. For spherical growth to be continuous, a sufficient number of vacancies must diffuse to the particle from sources such as dislocations, grain-boundaries and the surface of the specimen. However, the number of vacancies and their rate of supply to a growing particle decreases with decreasing temperature and increasing depth in single crystal material. This means that at sites well below the specimen

surface the concentration of vacancies is in general not sufficient to allow uniform radial growth, i.e. spherical growth. It is assumed that in this situation the growth of the particles will occur in certain preferred crystallographic directions. Experimental evidence supports this, in that for oxidation at 1000° C and below, the particles become more predominantly a mixture of cuboids and elongated cuboids with increasing depth of oxidation and their faces bear some simple relation to the crystal structure of the matrix. In fact the faces of the cuboids are parallel to {100} planes of the nickel (fig. 3). When all the silica has been precipitated, vacancies will still be supplied to the cuboidal particles allowing them to minimise their surface energy by rounding off into spheres. The vacancy concentration and mobility at oxidising temperatures of the order 800° C seem to be too low to sustain directional growth and the particles formed at this temperature have no regular shape. This low vacancy concentration is probably the reason for the silica film formation in that such films can be regarded as being a preferential growth in two <100> nickel directions parallel to the oxygen front, as opposed to the three-dimensional cuboid growth for the higher vacancy concentrations. The crystalline silica films formed at this teperature must be partially coherent with the nickel matrix and be due to precipitation in an extremely low vacancy concentration. The precipitation of thin films causes the minimum increase in strain energy in the matrix [20, 21]. The identification of these films is not as yet clear, but electron diffraction suggests that some may have a hexagonal, high temperature quartz or tridymite structure.

In polycrystalline material with its additional source of vacancies, e.g. grain-boundaries, the shape of the particles in the grains is usually spherical, although again some cuboidal forms are precipitated at greater depths below the specimen surface, for oxidising temperatures below 1000° C. The grain-boundaries also have a considerable effect on the oxidation rate of the Ni–0.058 wt % Si alloy in that the diffusion rate of oxygen along the boundaries above 1000° C is several times greater than that through the grains. This enhanced grain-boundary diffusion of oxygen is similar to that reported by Schenck *et al* [22] in Fe–Si alloys. Thus silica preferentially precipitates at the grain-boundaries because the supply of the reagents, oxygen, silicon and vacancies, is rapid. The size of the particles precipitated on the boundaries increases with increasing grain-boundary misorientation, possibly because of a corresponding increase in vacancy concentration, but is never greater than the average particle size in the grains and never less than 0.05 μm. The localised network growth which is often extended in a plane parallel to the oxidation front is assumed to occur at sites on the boundaries where the vacancy concentration is such that growth of existing structures is preferred to nucleation of other particles. This effect therefore occurs at the lowest temperatures and greatest depths where the oxidation front advances more slowly. The preferential precipitation at the grain-boundaries reduces the amount of silicon in the grains and so the size of the particles in the grain is smaller than those precipitated in the single crystal alloy at the same temperature.

The formation of the arrays of particles in the unannealed specimens is thought to be due to a greater concentration of vacancies than of reacting silicon and oxygen. The precipitation of filaments, which are analogous to the elongated cuboids in the single crystal material, would take place when there is a low vacancy concentration. The length of the filaments is usually less than 5 μm. The symmetry of the particle arrays and filaments suggests a growth process related to crystallographic directions in the grains or an isotropic competition for the reagents which produces a regular lattice of growth centres. The filaments occasionally provide sites for the growth of dendritic structures whose branches seem to be similar to the filaments in that they tend to grow in related directions (fig. 9). The more pronounced particulate nature of the precipitate in this unannealed alloy is consistent with the fact that there are many more vacancy sources.

The rates of oxidation in the Ni–0.48 wt % Si alloy are, as expected, much less than in the Ni–0.058 wt % Si alloy. In fact the same oxidation rates occur in the two alloys when the oxidising temperatures differ by approximately 75° C. In the surface region, where the velocity of the oxidation front and the vacancy diffusion rate are relatively fast compared with the diffusion rate of silicon, particles of silica are precipitated but when the reaction front velocity and the silicon diffusion become comparable the majority of the oxidation product is of a large scale filament type. Again it is assumed that this

filamentary structure forms because of a lack of vacancies. It is evident from fig. 11b that the filaments in a particular grain are crystallographically oriented in one direction and their branches are directed perpendicular to the main filament. From this observation and electron diffraction information it would seem that the main filaments lie in the <100> nickel direction nearest to the plane of the oxidation front and their branches are in other <100> directions. Spheroidisation of the ends of the filaments and their branches occurs when all the silica has been precipitated and the vacancy concentration increases again to the equilibrium value. Preferential precipitation occurs at the grain-boundaries to such an extent that they become saturated with silica as shown on the boundary in fig. 11b. The oxygen diffusing along the boundaries is thus impeded and the oxidation front advances as a plane, parallel to the specimen surface.

The rates of oxidation in the Ni–Co–Si alloy are less than those in the Ni–Si alloy containing three times the amount of silicon which indicates that the oxygen diffusion rate and/or the oxygen solubility are less in the Ni–Co alloys than in pure nickel. As the minimum particle size is greater than 0.1 μm it is apparent that the ratio of oxygen to silicon diffusion rates has a similar value to that determined for the nickel alloy. Figs. 12a and b show clearly the change in structure of the oxidation product with depth, and the intense grain-boundary precipitation at the greater depths. The fact that there is little preferential precipitation at grain-boundaries in the surface region suggests that the oxygen diffusion is not enhanced along the boundaries. The dendritic forms are similar in shape to those precipitated in the unannealed Ni–0.058 wt % Si alloy but they have much larger dimensions. However, unlike the Ni–Si case, they are all precipitated in the grains and are in no way related to the grain-boundaries.

5. Conclusion

It is evident from the results of this work that a well-defined precipitate system of spheroidal silica particles can be obtained in Ni and Co–Ni sections of thickness of the order 100 to 200 μm by internal oxidation at high temperatures. Such a system has obvious application to an experimental investigation of statistical theories of coercivity and magnetisation. Particles vary in size from about 0.2 μm to 0.5 to 1.0 μm in the low percentage silicon alloy and 0.2 μm to 1.0 to 2.0 μm in the higher percentage silicon alloys. Size distributions of this order will allow an investigation of how the mean size and distribution of particles, varied by oxidising different thicknesses of alloy, determine the coercivity and the approach to magnetic saturation in these systems.

The extended structures of silica, especially the very regular dendritic and branching forms, obtained throughout the high percentage polycrystalline silicon alloys oxidised at certain temperatures and depths, would offer considerable resistance to domain wall motion by subdivision of the alloy matrix into magnetically discrete regions with dimensions $\sim$ 15 μm and so cause increased magnetic coercivity and "squareness" of the hysteresis loop. The possible use of internally oxidised or dispersion-strengthened ferromagnetic alloys as device material in situations where creep resistance is required, e.g. in high temperature power systems, has been suggested [13, 23]. Investigation of the magnetic properties of dispersion strengthened Co, Fe and Ni showed that such materials have promising "soft" magnetic properties [13]. For high temperature use a fairly high saturation magnetisation value and Curie temperature are obviously required and hence internally oxidised or dispersion strengthened Co, Fe, Co–Fe and Co–Ni alloys are worthy of investigation.

It is hoped to extend this work to an investigation of internal oxidation in Fe and Co alloys and to measurement of the magnetic properties of these systems and of those reported on here.

Acknowledgement

The authors would like to thank Mr I. M. Stewart of the Nelson Research Laboratories, English Electric Co Ltd for the results obtained on the Stereoscan scanning electron microscope. Acknowledgements are due to the SRC for the award of a Research Studentship (R.B.) and to the Air Force Office of Scientific Research for support through the European Office of Aerospace Research, OAR United States Air Force under Grant EOOAR–68–005. The continuing interest of Professor R. S. Tebble in this work is appreciated.

References

1. L. NÉEL, *Ann. Univ. Grenoble* **22** (1946) 299.
2. E. KONDORSKY, *Dokl. Akad. Nauk SSSR* **68** (1949) 37.

3. W. D. NIX and R. A. HUGGINS, *Phys. Rev.* **135** (1964) A401.
4. L. J. DIJKSTRA and C. WERT, *ibid* **79** (1950) 979.
5. L. NÉEL, *J. Phys. Radium* **9** (1948) 184.
6. A. HUMPHREYS and P. RHODES, Proc. Int. Conf. on Magnetism, Nottingham (1964), p. 689.
7. E. SCHLÖMANN, *J. Appl. Phys.* **38** (1967) 5027.
8. S. L. CUNDY and P. J. GRUNDY, *Phil. Mag.* **14** (1966) 1233.
9. M. F. ASHBY and G. C. SMITH, *J. Inst. Metals* **91** (1962-63) 182.
10. O. PRESTON and N. J. GRANT, *Trans. AIME* **221** (1961) 164.
11. P. BOLSAITIS and M. KAHLWEIT, *Acta Metallurgica* **15** (1967) 765.
12. L. J. BONIS and N. J. GRANT, *Trans. AIME* **224** (1962) 308.
13. R. J. TOWNER, D. M. PAVLOVIC, K. DETERT, and A. S. BUFFERD, *J. Appl. Phys.* **39** (1968) 601.
14. F. N. RHINES, *Trans. AIME* **137** (1940) 246.
15. F. N. RHINES, W. A. JOHNSON, and W. A. ANDERSON, *Trans. AIME* Tech. Publ. No. 1368, (1941).
16. K. HAUFFE, "Oxidation of Metals" (Plenum Press, London, 1965).
17. C. J. SMITHELLS, "Metals Ref. Book", Vol. II (London, Butterworths, 1967), p. 670.
18. A. KELLY and R. B. NICHOLSON, *Prog. Mat. Sci.* **10** (1963) 285.
19. M. F. ASHBY and L. M. BROWN, *Phil. Mag.* **8** (1963) 1649.
20. N. NABARRO, *Proc. Roy. Soc.* **A175** (1940) 519.
21. R. G. BAKER, D. G. BRANDON, and J. NUTTING, *Phil. Mag.* **4** (1959) 1339.
22. H. SCHENCK, E. SCHMIDTMANN, and H. MULLER, *Arch. Eisenhüttenw* **31** (1960) 121.
23. A. C. BEILER, *J. Appl. Phys.* **38** (1967) 1161.